

## FIRST-SPIRE

### New proposal for photometer optical design

Kjetil Dohlen

dohlen@observatoire.cnrs-mrs-fr

Laboratoire d'Optique, Observatoire de Marseille  
2 Place Le Verrier, 13248 Marseille Cedex 4, France

## 1. Introduction

The original photometer proposed for SPIRE is reviewed and a different design is proposed, offering improved image and pupil quality. This is achieved at the cost of surface complexity and the appearance of distortion and variable focal ratio. The overall geometry of the system up until the cold stop is largely conserved.

## 2. Design criteria

We consider here design criteria concerning optical quality. Stray-light, beam clipping, thermal aspects and mechanical implementation are not considered.

Three optical design criteria may be defined:

- 1) **Final image quality:** We assume the Marechal criterion for diffraction limited optics, i.e. Strehl ratio  $S > 0.8$  ( $S = 1$  for perfect optics). This corresponds to an RMS wavefront error at  $\lambda = 200 \mu\text{m}$  of  $w = \lambda/13 = 15 \mu\text{m}$ . An error budget must be created taking into account the theoretical image quality of the instrument, FIRST telescope quality, manufacturing and alignment tolerances, etc. This has not been done for SPIRE yet. As a reasonable target for instrument optical quality we assume  $w < \lambda/20 = 10 \mu\text{m}$ .
- 2) **Intermediate image quality:** Since the spectrometer does not work in the same plane as the photometer, it is very unlikely that aberrations present in the intermediate focal plane can be corrected by the spectrometer optics. For a diffraction limited spectrometer image, the intermediate image must therefore be better than the final image, say  $w < 8 \mu\text{m}$ .
- 3) **Pupil image quality in the cold-stop:** The cold stop avoids detectors to see anything outside the telescope pupil. If the image of the pupil onto the cold stop suffers from aberrations, the pupil image is not the same for all points in the FOV. For the cold-stop to be efficient, it must then be undersized, producing a loss of signal. Again an error budget is required to take account of all the effects affecting this performance (diffraction, alignment, etc). For the present purposes we assume a requirement for the geometrical optical design of **< 10% loss of flux at the cold stop**.

## 3. Original design

The original design (Figure 1) uses a spherical tertiary (M3) to image the FIRST pupil (M2) onto a flat chopping mirror (M4). The chopper allows the instrument FOV to be swept across the telescope focal plane. A toroidal M5 reimages the focal plane onto an intermediate image in which is located a small pick-off mirror feeding the spectrometer channel. M5 also produces an image of the pupil, located just after the flat M6. The cold stop, materializing the limiting aperture for the instrument, is located in this pupil image. A toroidal M7 relays the star-space image onto the final focal plane, providing sufficient back-focal clearance to fit two dichroics mounted at  $25^\circ$  to the beam, thus feeding three individual detector arrays.

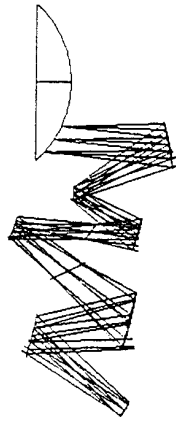


Figure 1. Present baseline design for the SPIRE photometer.

**Final image quality** is limited by the toroidal M7 which produces a nearly perfect image at the centre of the field but suffers from astigmatism at the edges (Figure 2 (a)). In the worst corner of a 5' x 5' FOV, **the wavefront error is 32  $\mu\text{m rms}$** . The specified 10  $\mu\text{m}$  is achieved within a circle of diameter 3'.

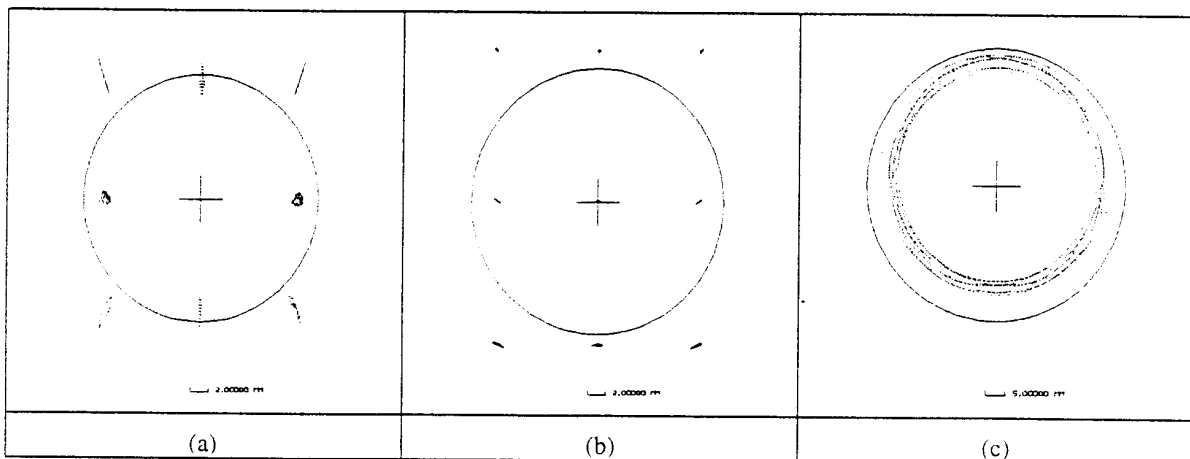


Figure 2. Raytracing results for the present baseline. (a): Final image spot diagrams for a 5' x 5' FOV. (b): Intermediate image spot diagrams. (c): Outline of the telescope pupil imaged onto the cold stop for several points in the field.

Image quality in the **intermediate focus** is within the specified **8  $\mu\text{m rms wavefront error}$**  (Figure 2(b)). The image plane is tilted 35° wrt optical axis.

**Pupil imaging** suffers from coma, producing an important blurring of the image of M2 upon the cold stop (Figure 2(c)). The walk of the M2 image in the cold-stop plane is about 5 mm and the diameter of the image is about 55 mm. The cold stop must therefore be reduced to a diameter of 50 mm to avoid leakage, hence inflicting a **light loss of 17%**.

## 4. New proposal

We realized that pupil imaging was improved by changing M3 into an off-axis parabola, creating nearly optimal imaging of the telescope pupil onto M4. Adjusting the toricity of M5 slightly ensured a good pupil image also in the cold-stop plane (Figure 4(c)), achieving a **light loss due to pupil undersizing of about 8%**. A loss of final image quality was observed, however. Replacing the flat M6 and toroidal M7 by a couple of off-axis paraboloids with a collimated beam between them (Figure 3) was found to preserve the good pupil image while giving excellent quality in the final image (Figure 4(a)) with **RMS wavefront errors less than 8  $\mu\text{m}$** . The intermediate image quality (Figure 4(b)) is still sufficient but its tilt is increased to about  $50^\circ$ . This increase in tilt appears to be due to the use of a parabolic M3. Its impact upon image quality in the spectrometer has not been assessed.

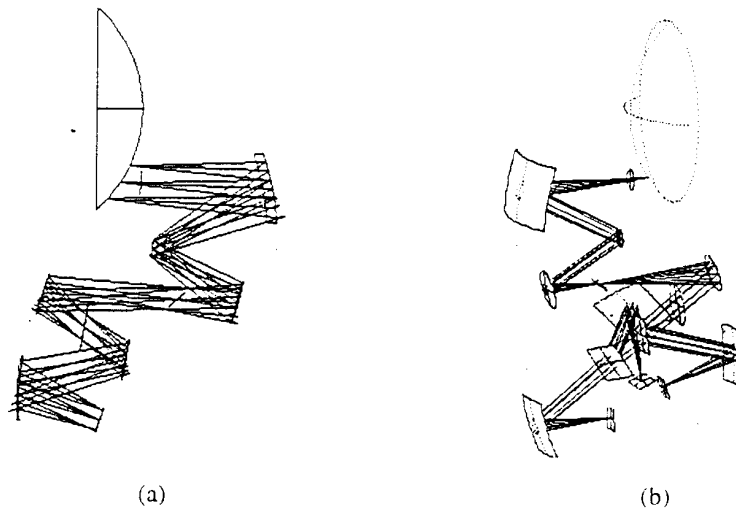


Figure 3. Proposed design for the SPIRE photometer. (a): Profile drawing with a single channel. (b): Perspective drawing with all three channels.

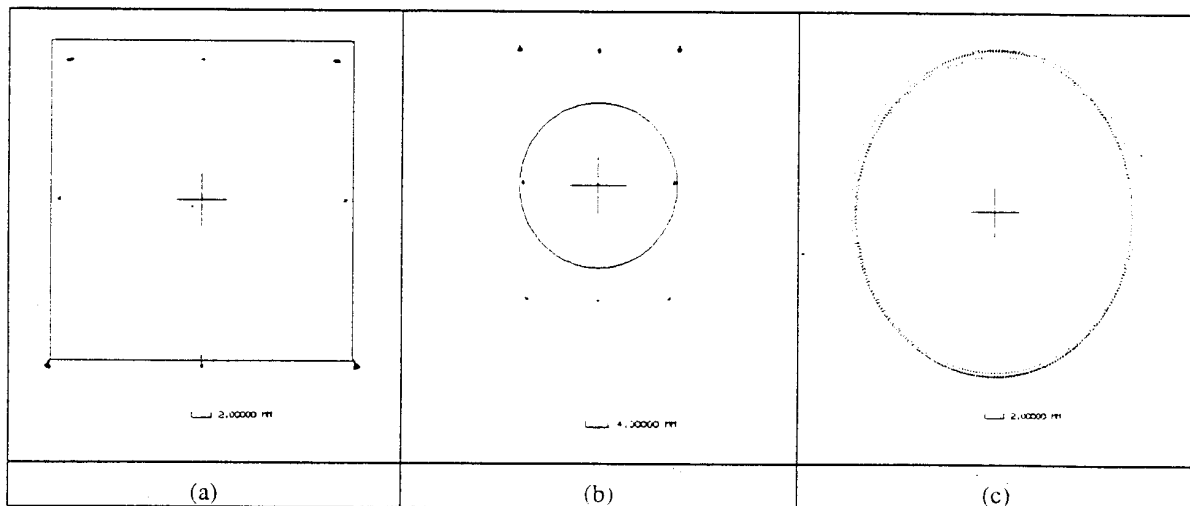


Figure 4. Raytracing results for the proposed design. (a): Final image spot diagrams for a  $5' \times 5'$  FOV. (b): Intermediate image spot diagrams. (c): Outline of the telescope pupil imaged onto the cold stop for several points in the field.

The main difference wrt the original design is that dichroics are located before rather than after M7. Each channel therefore has its own (parabolic) M7 focalizing the beam onto the detector arrays. The dichroics are mounted at  $25^\circ$  to the beam and one of them send the beam out into the plane perpendicular to the plane of the system. Figure 3(b) shows a 3D view of the complete system. The focal planes are located on three sides of an approximately rectangular box as indicated in Figure 5.

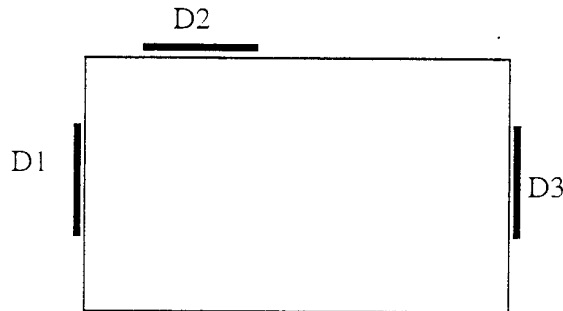


Figure 5. Arrangement of the three focal planes.

It is the use of off-axis parabolic M6 and M7 as final image relay and a cold-stop placed close to M6 which allows for the excellent image quality and the correction of the large image tilt, present in the system due to the curvature of the FIRST focal plane. The cost of this correction is a distorted image and a variable focal ratio. The distortion is illustrated in Figure 6, showing the image of a  $5' \times 5'$  object. Table 1 lists focal ratios for points A, B, and C in the FOV. Detector 1 behaves slightly better than the two others because the distance between M6 and M7 is shorter for this channel.

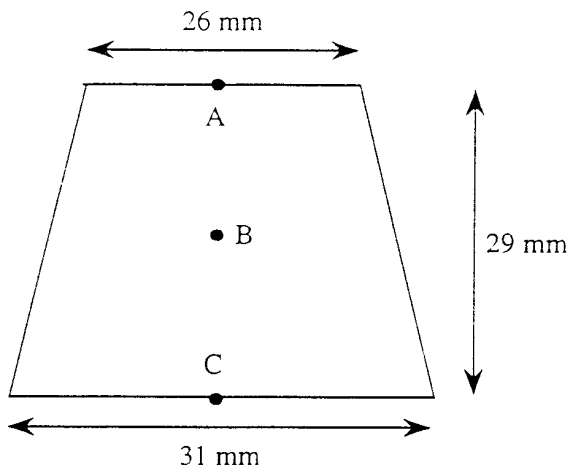


Figure 6. The image of a  $5'$  square object, illustrating the distortion of the final image. Points A, B, and C refer to Table 1.

Table 1. Tangential and sagittal focal ratios for the three points in the FOV named A, B, and C in Figure 1.

Point in FOV	Detector 1		Detectors 2 and 3	
	$F_{\text{tangential}}$	$F_{\text{sagittal}}$	$F_{\text{tangential}}$	$F_{\text{sagittal}}$
A (upper edge)	4.8	5.0	5.0	5.3
B (centre)	5.6	5.4	6.3	5.9
C (lower edge)	6.7	5.6	8.0	6.3

## 5. Conclusion

Optical design criteria and embryonic error budgets for the SPIRE photometer are presented. Comparison with the optical performance of the present baseline design indicates that it suffers from insufficient image and pupil quality. A new concept is proposed offering the required improvements. This is achieved at the cost of increased surface complexity and the introduction of distortion and variable focal ratio across the FOV. A scientific specification for the allowed variation in focal ratio is required in order to attempt a trade-off between scientific, optical, and mechanical performance.